Finite Element Analysis of Underwater Capacitor Micromachined Ultrasonic Transducers

Yongrae Roh, *Member, IEEE*, and Butrus T. Khuri-Yakub, *Fellow, IEEE*

Abstract—A simple electro-mechanical equivalent circuit model is used to predict the behavior of capacitive micromachined ultrasonic transducers (cMUT). Most often, cMUTs are made in silicon and glass plates that are in the 0.5 mm to 1 mm range in thickness. The equivalent circuit model of the cMUT lacks important features such as coupling to the substrate and the ability to predict cross-talk between elements of an array of transducers. To overcome these deficiencies, a finite element model of the cMUT is constructed using the commercial code ANSYS®. Calculation results of the complex load impedance seen by single capacitor cells are presented, then followed by a calculation of the plane wave real load impedance seen by a parallel combination of many cells that are used to make a transducer. Cross-talk between 1-D array elements is found to be due to two main sources: coupling through a Stoneley wave propagating at the transducer-water interface and coupling through Lamb waves propagating in the substrate. To reduce the cross-talk level, the effect of structural variations of the substrate are investigated, which includes a change of its thickness and etched trenches or polymer walls between array elements.

I. Introduction

CAPACITOR micromachined ultrasonic transducers (cMUT) are gaining acceptance as an alternative to piezoelectric transducers in many applications. They offer the advantage of increased bandwidth with comparable sensitivity to piezoelectric transducers as well as ease of fabrication and electronics integration [1]. The last decade has seen a large increase in the research effort on cMUTs. This is evidenced by the number of research groups throughout the world that are now investigating various aspects of cMUT design, performance, and manufacture [2]–[8]. Thus far, most of the design and analysis of cMUTs has been done using a simple Mason type equivalent circuit model to predict its behavior [1]. However, the equivalent circuit model lacks some important features such as the coupling into the substrate and the ability to predict cross-talk between elements of an array of transducers. Many applications, such as ultrasonic imaging, however, demand better understanding and improvement of cMUTs both in terms of individual device

performance and array behavior. Considering that cross coupling between elements is one of the most important factors affecting the performance of an array transducer [9], there is a strong need to develop a multi-dimensional analysis technique to identify the sources of the problem and the means to reduce its effect.

The basic physical structure of an immersion cMUT is a solid silicon plate with fluid on both sides. The boundary conditions associated with cMUTs provide the environment for the excitation and propagation of various spurious modes such as Lamb waves and Stoneley waves. Experimental evidence of the cross-talk in cMUTs was investigated and reported earlier [10]. Results of this work show that Lamb waves and Stoneley waves are the two main causes of cross coupling. Lamb waves refer to the elastic modes of propagation in a solid plate with free boundaries [11]. When Lamb wave modes propagate in a fluid-loaded silicon wafer, they may suffer leakage by mode conversion into the fluid at a radiation angle dictated by Snell's law. Due to the dispersive nature of Lamb waves, the radiation pattern of the Lamb waves in a silicon wafer will be a strong function of the plate thickness and frequency of operation. Stoneley waves propagate at the plane interface between two semi-infinite solids or the interface between a fluid and a semi-infinite solid [11]. At the interface between a fluid and an elastic solid, two kinds of surface waves can propagate. One is the leaky Rayleigh wave; the other is the Stoneley wave [12]. These two waves are quite different from each other in that most of the acoustic energy of the Stoneley wave resides in the fluid, and that of the leaky Rayleigh wave resides in the solid. The Stoneley wave is nonattenuative and propagates at the speed of the sound velocity in the fluid medium. The leaky Rayleigh wave attenuates by leaking into the fluid and propagates at the constant surface wave velocity of the solid medium. This undamped, nearly nondispersive Stoneley wave can cause significant cross coupling because it will carry the energy directly from an active cMUT array element to its nonactive neighboring elements.

In this study, finite element analyses are performed to investigate the cross coupling mechanism in cMUTs. A two-dimensional finite element model of the cMUT is constructed using the commercial code ANSYS®. Through various analyses with the model, we analyze the origin and level of the cross-talk between array elements, with evidence of coupling through Stoneley waves propagating at the transducer-water interface and coupling through

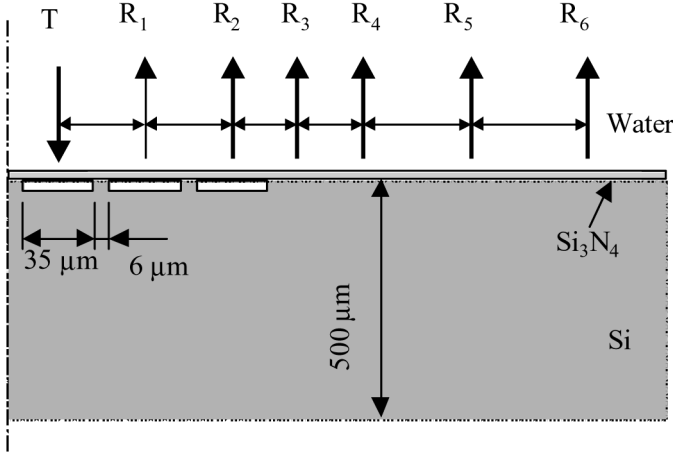Fig. 1. Schematic view of an underwater single cMUT transducer on a Si wafer.

Fig. 2. Finite element model of the underwater single cMUT transducer on a silicon wafer.

Lamb waves propagating in the wafer. Furthermore, for the reduction of the cross-talk level, the effects of various structural schemes are investigated. These include change of wafer thickness and placement of etched trenches in the wafer to prevent the cross coupling through Lamb waves, as well as placement of acoustic walls between elements to prevent the cross coupling through Stoneley waves.

II. Finite Element Model of a Single cMUT Cell

As a first step to investigate the cross-talk mechanism, a single cMUT transducer is modeled with the ANSYS as shown in Fig. 1. In Fig. 1 we note one transmitter cMUT made of a single capacitor cell and two receivers made similarly of single capacitor cell cMUT at the surface of a silicon wafer. The geometry of the three cMUTs is the same. Each consists of a silicon nitride (Si_3N_4) membrane of 0.8 μm thickness and 35 μm diameter and a vacuum gap of 0.15 μm depth in the wafer. This whole solid structure is immersed in water. The transmitter cMUT is excited by a surface pressure distributed over the center half of its membrane surface. The cross-talk pressure and displacement are measured in response to the excitation at various points denoted R on the silicon surface, two of which are over the receiver cMUTs, and several are over the silicon surface where no cMUTs are placed. Thus, we study the continuing propagation of spurious modes past the cMUTs. The excitation pressure is applied in the form of a square pulse signal.

Fig. 2 shows the finite element model of the structure in Fig. 1. The silicon wafer is chosen to be 4 mm long and 0.5 mm thick. The circumference of the water is enforced by infinite boundary conditions in order to avoid the limit imposed by the finite dimensions in the model. The whole model consists of 26,500 nodes and 26,300 elements. The model is built with the adaptive meshing technique so that high enough accuracy can be maintained in analyzing the micro-motion of the Si_3N_4 membrane with minimal calculation time.
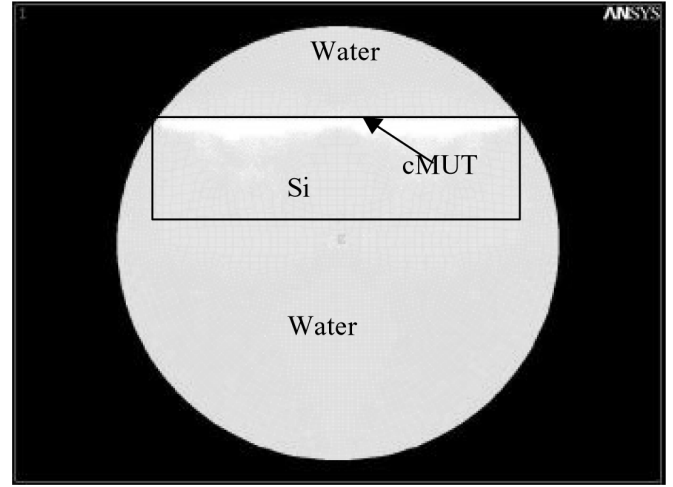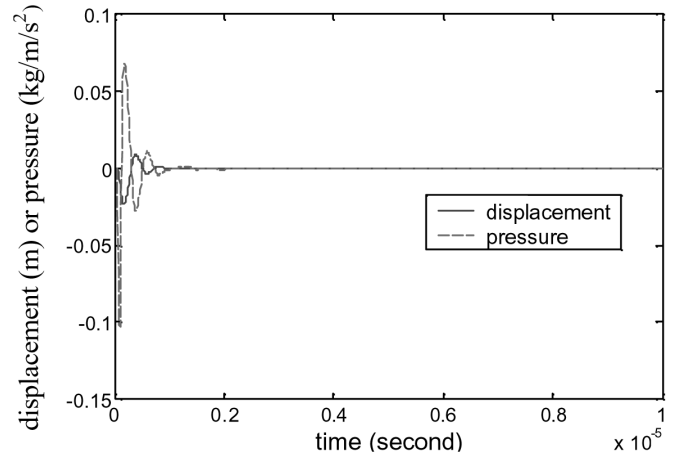

Fig. 3. Transient responses of the receiver cMUT, R_1, in Fig. 1.

With the model, various time domain and frequency domain responses of the structure are obtained through transient and harmonic analyses. Fig. 3 and 4 are results of the transient and harmonic analyses, respectively. These responses of the receiver cMUT in relation to the excitation pressure allow the analysis of the cross-talk mechanism. The load impedance of each transmitter and receiver cMUT in Fig. 1 also can be calculated from the frequency spectrum of displacement and pressure, and the results are shown in Fig. 5.

Fig. 5(a) shows that the transmitter cMUT has a load impedance that is complex (solid line). The complex load impedance means that the transmitter cMUT works almost like a point source due to its small dimension in comparison to the wavelength. The theoretical complex impedance (dotted line) of a circular piston on an infinite baffle is also shown in Fig. 5 and is compared with the numerical data [13]. The good agreement between the numerical and theoretical values verifies the validity of the finite element model, and proves that there is a direct relationship between the excitation pressure and the ex-
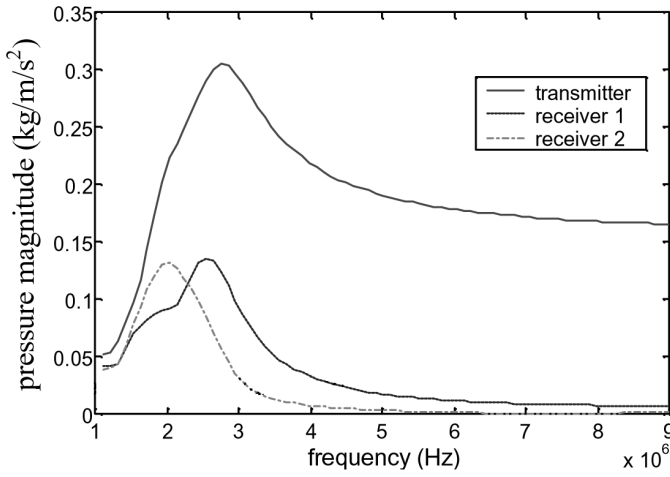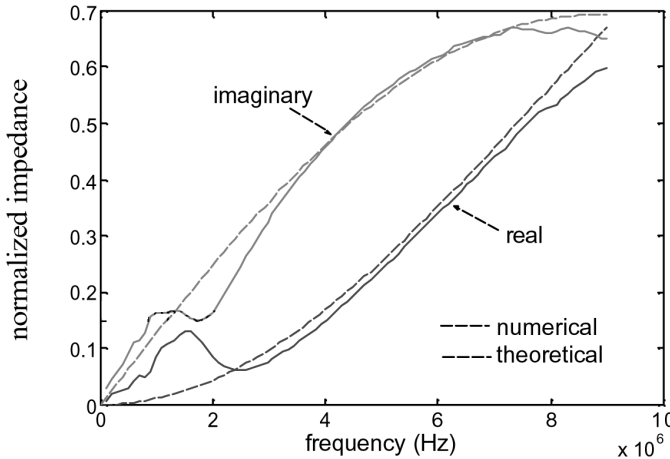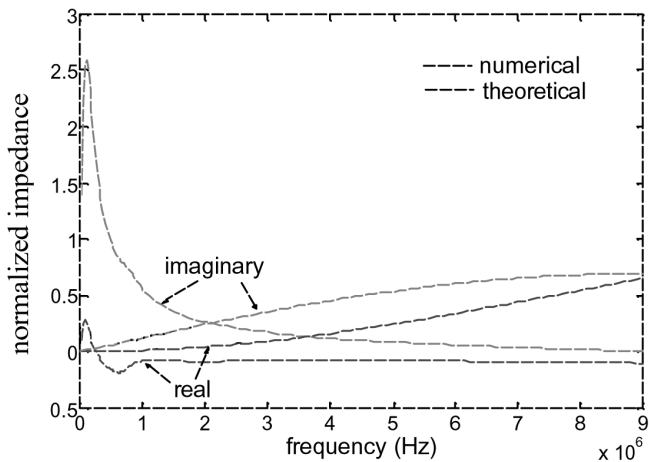

Fig. 4. Frequency responses of the three cMUTs, T, R_1, and R_2, in Fig. 1.

(a) transmitter cMUT (T)

(b) receiver cMUT (R_1)

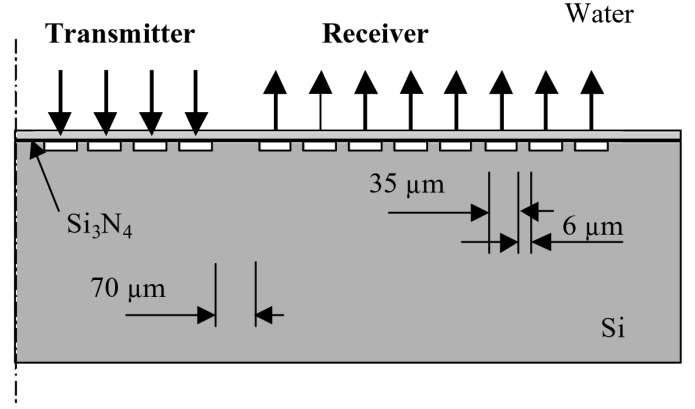Fig. 5. Radiation impedance z of a single cMUT cell.

Fig. 6. Schematic view of an underwater cMUT array transducer.

cited displacement. However, in Fig. 5(b), the numerical complex impedance of the receiver cMUT does not show any agreement with the theoretical value, which means that the cross-talk pressure has no cause-and-effect relationship with the cross-talk displacement. This result indicates that the cross-talk pressure and the displacement at the receiver cMUT are not coupled with each other, and each field has its own means of energy transport. According to the temporal analysis results in Fig. 3, the pressure field propagates from the transmitter cMUT to the receiver cMUTs at the speed of the sound velocity in water (1,480 m/s). Therefore, this result and the experimental results reported earlier [10] show that the Stoneley wave propagating along the transducer-water interface is responsible for the cross-talk pressure. Similarly, the propagation speed of the displacement field (3,660 m/s) and the previous experimental results [10], [14] prove that the Lamb wave propagating in the Si wafer is responsible for the cross-talk membrane displacement.

III. FINITE ELEMENT MODEL OF A CMUT ARRAY

A finite element model is also constructed for an underwater cMUT array transducer. Fig. 6 is the schematic diagram of the array transducer. The geometry and materials of each cMUT in the array are the same as those of the single cMUT cell in Section II. Eight cMUTs are combined in parallel to make either a transmitter array element or a receiver array element. The excitation condition for each cMUT in the transmitter is the same as before. All eight cMUTs in the transmitter array element are excited simultaneously to represent the parallel connection, and the responses of the receiver array element are investigated in relation to the behavior of the transmitter array. The mechanical responses of each cMUT in the receiver array are averaged to simulate their electrical parallel connection. With the model, similar analyses are performed as for the single cell cMUT. The load impedance of the transmitter array is calculated and compared with the theoretical radiation impedance of a circular piston of the same radius on an infinite baffle and are presented in Fig. 7.
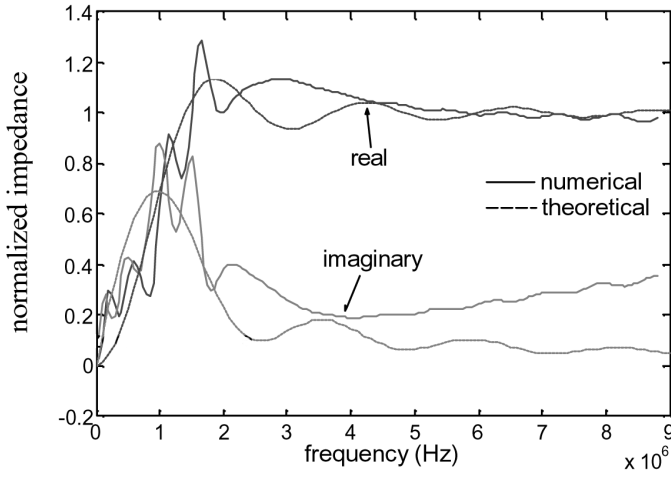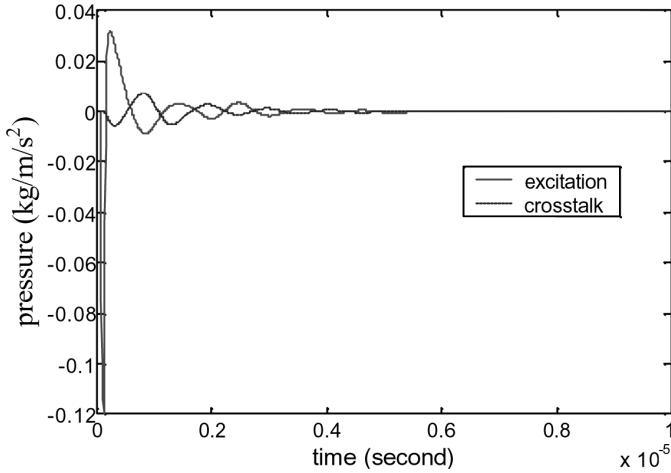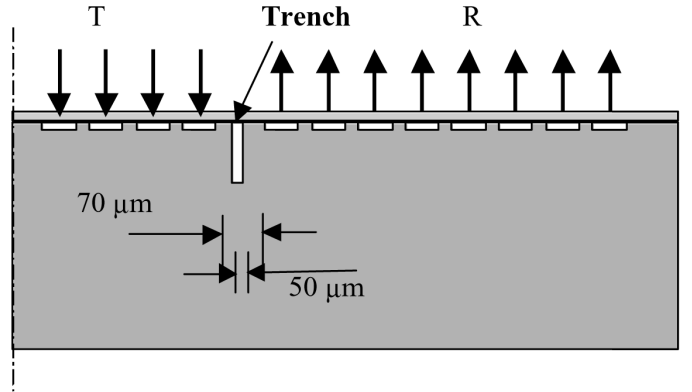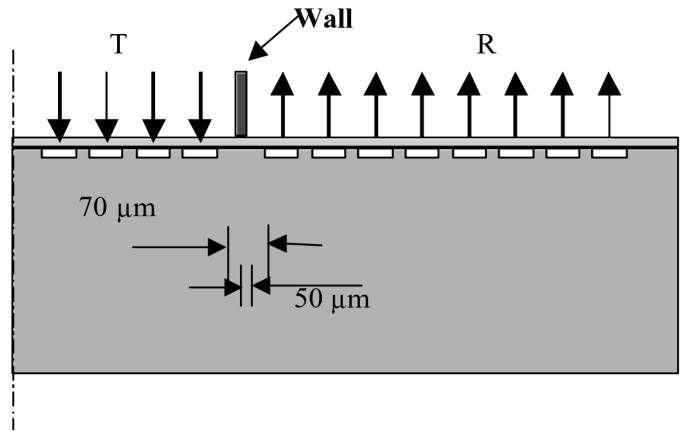
Fig. 7. Radiation impedance z of a cMUT array.

(a) trench

Fig. 8. Excitation pressure and cross-talk pressure for the cMUT array in Fig. 6.

(b) wall

Fig. 9. Schematic view of the cross-talk control structures.

IV. CROSS-TALK CONTROL STRUCTURES

The whole structure of the array is more complicated than the single cMUT, which leads to more discrepancy from the behavior of a pure circular piston. However, in general, the numerical impedance shows a fairly good agreement with the theoretical value, which verifies the validity of the finite element array model, again. The array transducer is composed of eight cMUTs connected in parallel and has much bigger radius than the single cMUT. Hence, the real part of the impedance is more dominant in Fig. 7, which means that the array element transducer behaves more like a plane piston than the single cell cMUT. The finite element model also allows us to analyze the transient and harmonic responses of the array transducer. As an illustrative result, Fig. 8 is the excitation pressure applied to the transmitter array and the cross-talk pressure observed at the receiver array. The Fig. 8 confirms that cross-talk exists between the transmitter array and the receiver array. The level of the cross-talk in Fig. 8 is −22.6 dB.

Cross coupling between elements is one of the most important factors affecting the performance of an array transducer [2]. Since the cross coupling between array elements has been confirmed through the analyses in Section III, several structural schemes were investigated to reduce the cross-talk level. First, we investigated the effect of changing the thickness of the silicon wafer; second, we investigated the effect of placing an etched trench between the array elements; third, we investigated the placement of a wall of a polymer between the array elements. Fig. 9 shows the configurations of the trench and the wall. The first two schemes are an attempt to reduce the effects of the Lamb wave because the Lamb wave propagates inside the solid wafer. The third scheme was tried to reduce the effects of the Stoneley wave because most of the Stoneley wave energy resides in the water.
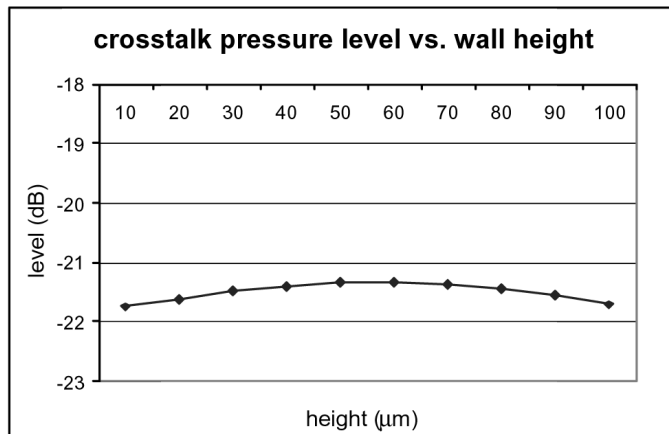
For each of the structural schemes, the same finite element analyses as before are performed to assess the effectiveness of each structure. The influences of these struc-
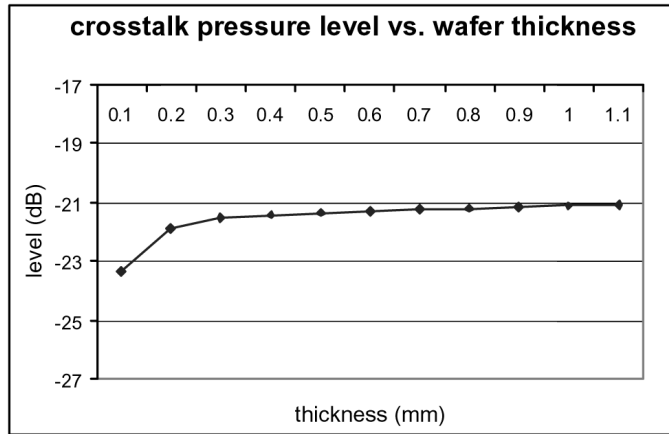
(a) change of wafer thickness
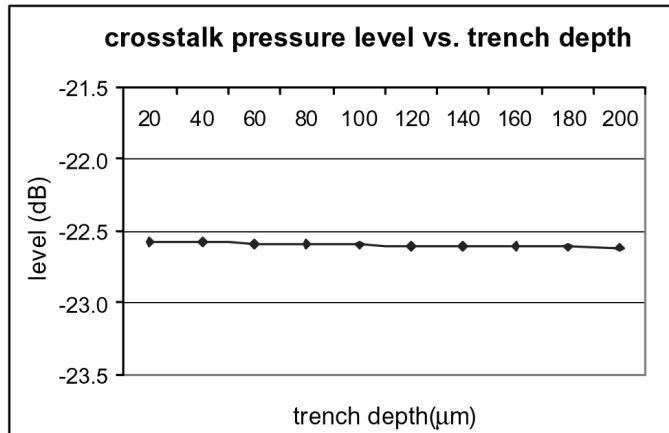
(b) change of trench depth

(c) change of wall height

Fig. 10. Effects of cross-talk control structures.

tural variations are shown in Fig. 10. Fig. 10(a) is the variation of the cross-talk pressure level in relation to the change of wafer thickness. The cross-talk level increases with the thickness of the wafer, although the effect is not very strong. As the wafer is made thicker, the Lamb wave leaks more energy into water due to the change of its velocity that corresponds to the change of its critical angle. According to this result, a thinner wafer is more desirable for cross-talk reduction. However, when practical conditions for transducer fabrication are considered, there is a certain limitation in reducing the wafer thickness. Fig. 10(b) shows the variation of the cross-talk pressure level in relation to the change of trench depth. In the finite element model, the inside of the trench is set to be vacuum, and the width of the trench is fixed to be 50 μm. In Fig. 10, up to the depth of 200 μm for a 0.5 mm thick wafer, the trench is shown to have almost no effect in reducing the cross-talk level. Because only a portion of the wafer thickness is etched, the Lamb wave propagates as well as without the trench, and thus no reduction in the level. Deeper and wider trenches may help decrease the cross-talk level, but they may cause structural weakness of the transducer or change of the transducer radiation pattern. Hence, effectiveness of the trenches is not confirmed in this work. Fig. 10(c) shows the variation of the cross-talk pressure level in relation to the change of wall height. The wall is made of a common lossy polymer, polyurethane, and the width is fixed to be 50 μm. The wall was placed to perturb the propagation of the Stoneley wave. However, we can observe the cross-talk level to increase up to some height of the wall, and then to decrease after that. Careful analysis of the wall motion shows that a higher wall is likely to have its own vibration when the transmitter array is excited and thus generate its own pressure field. The effect of the wall motion results in a worse cross-talk level as noted in Fig. 10(c). However, with further increase of the height, the role of the acoustic fence to block the wave propagation becomes more prominent, and the resultant cross-talk level decreases. Hence, this result says that a well designed wall, such as a wall around each cell, can be an efficient tool to prevent the cross-talk between the arrays by the Stoneley wave, but it requires more elaborate design for optimal performance.

V. Conclusion

In this paper, using finite element models of cMUTs, we analyzed the origin and level of cross-talk between single cell elements as well as between array elements, with evidence of coupling through Stoneley waves and Lamb waves. The Stoneley wave was found to be responsible for the cross-talk pressure field, and the Lamb wave was responsible for the cross-talk displacement field, respectively. Based on the analyzed mechanism, several structural variations of the silicon wafer were tried to reduce the cross-talk level, and their effects were investigated. Of the three structural schemes, placement of a wall between the array

elements was found to be the most promising method to control the cross-talk; trenches between the array elements did not show any evidence of cross-talk level reduction. Further work will be pursued to elaborate the results in this paper, and that will lead to optimal design of cMUT structures robust to cross-talk.

References

[1] I. Ladabaum, X. C. Jin, H. T. Soh, A. Atalar, and B. T. Khuri-Yakub, "Surface micromachined capacitive ultrasonic transducers," *IEEE Trans. Ultrason., Ferroelect., Freq. Contr.*, vol. 45, p. 678, May 1998.
[2] K. Suzuki, K. Higuchi, and H. Tanigawa, "A silicon electrostatic ultrasonic transducer," *IEEE Trans. Ultrason., Ferroelect., Freq. Contr.*, vol. 38, p. 620, Nov. 1998.
[3] M. Haller and B. T. Khuri-Yakub, "A surface micromachined electrostatic ultrasonic air transducer," in *Proc. IEEE Ultrason. Symp.*, p. 1241, 1994.
[4] D. W. Schindel, D. A. Hutchins, L. Zoou, and M. Sayer, "The design and characterization of micromachined air coupled capacitance transducers," *IEEE Trans. Ultrason., Ferroelect., Freq. Contr.*, vol. 42, p. 42, May 1995.
[5] A. G. Bashford, D. W. Schindel, and D. A. Hutchins, "Micromachined ultrasonic capacitance transducers for immersion applications," *IEEE Trans. Ultrason., Ferroelect., Freq. Contr.*, vol. 45, p. 367, Mar. 1998.
[6] S. P. Kelly, R. Farlow, and G. Hayward, "Applications of through-air ultrasound for rapid NDE scanning in the aerospace industry," *IEEE Trans. Ultrason., Ferroelect., Freq. Contr.*, vol. 43, p. 581, Jul. 1996.
[7] H. Kapels, T. Scheiter, C. Hierold, R. Aigner, and J. Binder, "Cavity pressure determination and leakage testing for sealed surface micromachined membranes: A novel on-wafer test method," in *Proc. Eleventh Annu. Int. Workshop Micro Electro Mechanical Syst.*, p. 550, 1998.
[8] A. Caronti, G. Caliano, A. Iula, and M. Pappalardo, "Electrical impedance mismatch in capacitive micromachined ultrasonic transducers," in *Proc. IEEE Ultrason. Symp.*, 2000.
[9] J. D. Larson, "Non-ideal radiators in phased array transducers," in *Proc. IEEE Ultrason. Symp.*, p. 673, 1981.
[10] X. C. Jin, F. L. Degertekin, S. Calmes, X. J. Zhang, I. Ladabaum, and B. T. Khuri-Yakub, "Micromachined capacitive transducer arrays for medical ultrasound imaging," in *Proc. IEEE Ultrason. Symp.*, p. 1877, 1998.
[11] B. A., *Acoustic Fields and Waves in Solids.* 2nd ed. vol. 1, Malabar, FL: R. E. Krieger Publishing, 1990.
[12] H. Uberall, "Surface waves in acoustics," in *Physical Acoustics.* vol. 10, W. Mason and R. Thurston, Eds. New York: Academic, 1973, ch. 1.
[13] A. D. Pierce, *Acoustics: An Introduction to Its Physical Principles and Applications.* New York: McGraw-Hill, 1981.
[14] F. L. Degertekin, A. Atalar, and B. T. Khuri-Yakub, "Single mode lamb wave excitation in thin plates by hertzian contacts," *Appl. Phys. Lett.*, vol. 69, p. 146, Jul. 1996.

Yongrae Roh (S'88–M'91) was born in Taegu, Korea, on November 16, 1961. He received the B.S. and M.S. degrees in mineral and petroleum engineering from Seoul National University, Korea, in 1984 and 1986, respectively. He received the Ph.D. degree in engineering science and mechanics from the Pennsylvania State University, in 1990.

In 1990, he joined the Research Institute of Industrial Science & Technology as a senior research scientist and worked on the development of various piezoelectric devices. Since 1994, he has been with Kyungpook National University, Korea, where he is an associate professor in the Department of Mechanical Engineering.

Major research areas include ultrasonic transducers and SAW devices. He received the Xerox Award, USA, for the best researches in materials in 1990.
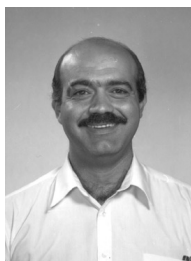
Butrus T. Khuri-Yakub (S'70–S'73–M'76–SM'87–F'95) was born in Beirut, Lebanon. He received the B.S. degree in 1970 from the American University of Beirut, the M.S. degree in 1972 from Dartmouth College, and the Ph.D. degree in 1975 from Stanford University, all in electrical engineering.

He joined the research staff at the Edward L. Ginzton Laboratory of Stanford University in 1976 as a research associate. He was promoted to a senior research associate in 1978, and to a professor of electrical engineering (research) in 1982. He has served on many university committees in the School of Engineering and the Department of Electrical Engineering. Presently, he is the Deputy Director of the Edward L. Ginzton Laboratory. Professor Khuri-Yakub has been teaching both at the graduate and undergraduate levels for over 15 years, and his current research interests include in-situ acoustic sensors (temperature, film thickness, resist cure, etc.) for monitoring and control of integrated circuits manufacturing processes, micromachining silicon to make acoustic materials and devices such as airborne and water immersion ultrasonic transducers and arrays, and fluid ejectors, and in the field of ultrasonic nondestructive evaluation and acoustic imaging and microscopy.

Professor Khuri-Yakub is a fellow of the IEEE, a senior member of the Acoustical Society of America, and a member of Tau Beta Pi. He is associate editor of *Research in Nondestructive Evaluation,* a journal of the American Society for Nondestructive Testing. He has authored over 300 publications and has been principal inventor or co-inventor of 40 issued patents. He received the Stanford University School of Engineering Distinguished Advisor Award, June 1987; the Medal of the City of Bordeaux for contributions to NDE, 1983; Acoustical Society of America Distinguished Lecturer Award, "Smart Structures and Microelectromechanical Systems (MEMS)," presented at the 138th Meeting of the Acoustical Society of America, Columbus, Ohio (November 1–5, 1999).